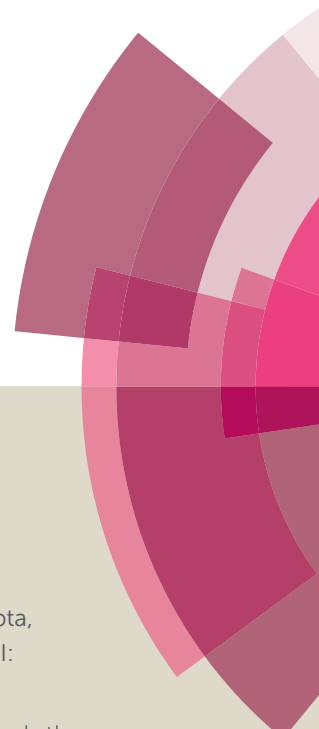


Catalysis Science & Technology

Accepted Manuscript



This article can be cited before page numbers have been issued, to do this please use: R. K. Rai, K. Gupta, D. Tyagi, A. Mahata, S. Behrens, X. Yang, Q. Xu, B. Pathak and S. K. Singh, *Catal. Sci. Technol.*, 2016, DOI: 10.1039/C6CY00037A.



This is an *Accepted Manuscript*, which has been through the Royal Society of Chemistry peer review process and has been accepted for publication.

Accepted Manuscripts are published online shortly after acceptance, before technical editing, formatting and proof reading. Using this free service, authors can make their results available to the community, in citable form, before we publish the edited article. We will replace this *Accepted Manuscript* with the edited and formatted *Advance Article* as soon as it is available.

You can find more information about *Accepted Manuscripts* in the [Information for Authors](#).

Please note that technical editing may introduce minor changes to the text and/or graphics, which may alter content. The journal's standard [Terms & Conditions](#) and the [Ethical guidelines](#) still apply. In no event shall the Royal Society of Chemistry be held responsible for any errors or omissions in this *Accepted Manuscript* or any consequences arising from the use of any information it contains.

Access to highly active Ni-Pd bimetallic nanoparticle catalysts for C-C coupling reactions

View Article Online
DOI: 10.1039/C6CY00037A

Rohit K. Rai,^a Kavita Gupta,^a Deepika Tyagi,^a Arup Mahata,^a Silke Behrens,^b Xinchun Yang,^c Qiang Xu,^c Biswarup Pathak^a and Sanjay K. Singh^{*a,d}

^aDiscipline of Chemistry, Indian Institute of Technology (IIT) Indore, Simrol, Indore, 452020, India

^bInstitute of catalysis Research and Technology (IKFT), Karlsruhe Institute of Technology (KIT), Hermann-von-Helmholtz-Platz 1, 76344 Eggenstein-Leopoldshafen, Germany

^cNational Institute of Advanced Industrial Science and Technology (AIST), Ikeda, Osaka 563-8577, Japan

^dCentre for Material Science and Engineering, Indian Institute of Technology (IIT) Indore, Simrol, Indore, 452020, India

Abstract

Bimetallic Ni-Pd alloy nanoparticles with high Ni to Pd atomic ratios (99:1 or 95:5) were prepared and the catalytic performances of these nanoparticle catalysts were explored for C–C coupling reactions (Suzuki-Miyaura, Heck and Sonogashira reactions) at moderate reaction conditions. In contrary to the monometallic, significantly enhanced catalytic activity was achieved with studied Ni-Pd nanoparticle catalysts for the C-C coupling reactions and achieved moderate to high yields. The turnover number (TON) increases with the increase in Ni to Pd atomic ratio for Ni-Pd nanoparticle catalysts, and can reach 3.6×10^3 for Ni_{0.99}Pd_{0.01} nanoparticle catalysed Suzuki-Miyaura reaction of arylbromides with arylboronic acid at 50 °C. Advantageously, such Ni-Pd nanoparticle catalysts with high Ni to Pd atomic ratios not only show significantly enhanced catalytic activity, but are also stable (ICP-AES analysis showing only marginal or absence of Pd leaching) and retain their catalytic activities for several catalytic runs (>90% conversion even at 7th catalytic run). Experimental and the relevant theoretical calculation (net charge localization using first principles calculations) suggested a substantial Ni to Pd charge transfer which resulted in a highly negatively charged

Pd centre, a favourable site for facile oxidative addition of arylhalides, and hence enhanced catalytic activity for Ni-Pd nanoparticle catalysts.

[View Article Online](#)
DOI: 10.1039/C6CY00037A

1. Introduction

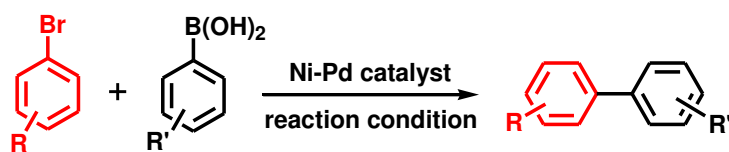
Heterogeneous catalysts based on bimetallic systems have received enormous scientific and industrial attention due to the superior catalytic performance shown by them compared to their monometallic counterparts.^{1,2} Significant synergic and cooperative interactions between the individual metal components, which involves fine tuning of metal-metal bonds in the hybrid state (structural tuning), transfer or exchange of electrons between the metals (electronic tuning), along with adsorption and stabilization of reactants and intermediates, accounts for the enhanced catalytic activity of these bimetallic nanoparticle catalysts.^{1,2}

Pd metal based catalysts have been the first choice for C–C coupling reactions.³ However, recent findings evidenced the extensive efforts made towards the development of Pd-based bimetallic nanoparticle catalysts, such as Pd-Au, Pd-Ag, Pd-Rh, Pd-Ru, Pd-Cu, Pd-Co or Pd-Ni, for several C-C coupling reactions, such as Suzuki-Miyaura reaction, Heck reaction, Sonogashira reaction, etc.⁴⁻¹² Because these bimetallic nanoparticle catalysts are not only found to be high performing catalysts, than their counterparts by overcoming their drawbacks, such as stability problems due to facile Pd leaching, but are also less-expensive, particularly those involving inexpensive and abundantly available non-noble metals (Pd-Cu, Pd-Ni or Pd-Co nanoparticle catalysts).³⁻¹² In near past, several reports appeared on the development of less expensive yet highly active bimetallic nanoparticle catalysts based on Pd-Ni, Pd-Cu, Pd-Co and so on.⁶⁻¹² Considering earlier investigations on bimetallic Pd-M (M = non-noble metals) catalysts, it is well documented that when a non-noble metal placed in close proximity of Pd, it will have a significant influence on the electronic structure of the Pd and therefore the Pd based bimetallic catalyst due to the electron transfer effect driven by the

differences in the electronegativity of the two metals. De *et al.* have also investigated the cooperative catalytic effect of Ni and Pd in the Ni-Pd (Ni to Pd atomic ratio 1:1) nanoparticles doped on mesoporous SiO₂ film for the Suzuki-Miyaura reaction at 50 °C in water-acetonitrile solution.⁹ XPS analysis of Ni-Pd catalyst where peaks corresponding to Pd⁰ was only observed along with the Ni²⁺ and Ni⁰ species, De *et al.* claimed the transfer of electron from Ni to Pd which keeps Pd in zero oxidation state and electron rich for facile oxidative addition of arylhalides. Recently, Ni-Pd nanoparticles supported on MWCNTs with varying Ni to Pd atomic ratios were investigated for the catalytic C-C coupling reactions and achieved quantitative yields of the biaryls products with Ni₅₀Pd₅₀ nanoparticle catalyst at 120 °C in water using TBAB as an additive.^{10a} Similarly Zu *et al.* have also investigated the Ni₅₀Pd₅₀ alloy nanoparticles for Heck reaction and achieved quantitative yields of the coupled products in DMF at 140 °C.¹¹ Similar electronic modification was also reported to be responsible for high activity for other analogous catalytic models for diverse catalytic reactions.^{13,14} Tsang *et al.* have reported Fe-Pd nanoparticles for C-C cleavage reaction and speculate that when Fe was placed in the close proximity of Pd, the lower electronegativity of Fe drive the electron flow to Pd.¹³ Zhao *et al.* have also observed an analogous enhancement in the catalytic activity due to the transfer of electron from Ni to Ru in the bimetallic Ni-Ru nanoparticle catalysts for hydrogenation and dechlorination reactions.¹⁴ Despite the fact that there is an enhancement in the catalytic activity in the bimetallic nanoparticle catalysts, in-depth investigations of the influence of the composition of the various components of the bimetallic nanoparticles on their catalytic properties is seldom reported. Recently, Metin and Sun *et al.* have explained graphene supported Ni/Pd core-shell nanoparticle with minimum Pd content (Ni to Pd ratio of 3:2) for Suzuki reaction of arylboronic acid and aryl halides at 110 °C in DMF: H₂O (7:3) using K₂CO₃ as a base.^{10b} For the synthesis of core-shell Ni/Pd nanocatalyst, they used Ni nanoparticles as a template which serves as a sacrificial reducing agent (transfer of electron from Ni to Pd due to difference in the reduction potential) for the

View Article Online
DOI: 10.1039/C6CY00037A

Pd salt and initiates Pd nucleation on the Ni surface. They anticipated that the high activity of the G–Ni/Pd catalyst is due to the good dispersion of G (graphene) in the *N,N*-dimethylformamide (DMF)-water mixture which helps to adsorb the aromatic component in the reactant through π – π interaction between graphene and aromatic ring of the reactant which brings them in close proximity of G–Ni/Pd nanocatalyst. High resolution TEM image of the G–Ni/Pd catalyst also revealed the appearance of lattice fringes having distance of ~0.232 nm analogous to the lattice spacing of the (111) planes of *fcc* Pd crystal (0.223 nm). Moreover, the high resolution elemental mapping of the Ni/Pd nanoparticles of 10 nm size showed the Ni atom centred at the core (~7.4 nm) and Pd (~1.3 nm) at the surface. Though the exposed surface of Ni/Pd nanoparticle is covered with Pd atom, the presence of the Ni metal core might have also contributed in the observed high catalytic activity of the G–Ni/Pd catalyst by synergistic effect bringing by possible Ni to Pd electron transfer. Analogous electron charge transfer, as observed in core-shell Ni/Pd nanoparticles,^{10b} is also expected for alloy Ni-Pd nanoparticles, where the Ni to Pd atom interactions are more prominent. In one of our recent findings about Ni-Pd nanoparticle catalysts for Suzuki-Miyaura reaction of arylhalides with arylboronic acids, we demonstrated a significant correlation between the Ni to Pd atomic ratios in the bimetallic Ni-Pd nanoparticle catalysts and their catalytic activities.¹² Remarkable enhancement in the catalytic activity of the Ni-Pd nanoparticle catalyst was observed with an increase in the Ni to Pd atomic ratio in the Ni-Pd nanoparticles. It was anticipated that due to the difference in the relative standard reduction potentials of Ni and Pd, probably, there is a natural transfer of electrons from Ni to Pd, resulting in the electron rich Pd centre which is expected to be a favourable site for facile oxidative addition of arylhalide. These significant findings raise several obvious questions: if this effect can further be extended to Ni-Pd nanoparticles with even higher Ni to Pd atomic ratios (99/1 or 95/5), and can be applied to other analogous catalytic C-C coupling reactions?

**Our work**

Ni to Pd molar ratio = 99:1	TOF = 3600 h ⁻¹
95:5	TOF = 540 h ⁻¹
90:10 (Ref. 12)	TOF = 75 h ⁻¹
Water-C ₂ H ₅ OH (v/v 1:1), T = 50 °C	

Previous reports**Cazorla-Amoros *et al.*, 2015** (Ref 10a)

Ni to Pd atomic ratio = 50:50	TOF = 990 h ⁻¹
Water, T = 100~120 °C	

Li *et al.*, 2011 (Ref 8a)

Ni to Pd atomic ratio = 50:50	TOF = 46 h ⁻¹
Dioxane, T = 100 °C	

Scheme 1 Bimetallic Ni-Pd nanoparticle catalysts for Suzuki-Miyaura reaction of aryl bromides and arylboronic acids.

To answer these, herein, we investigate the above assumption by increasing the Ni to Pd atomic ratios to 99:1 or 99:5 in the Ni-Pd nanoparticle catalysts and study its effect on the catalytic activity for Suzuki-Miyaura reaction (Scheme 1). To further explore the scope of this effect, the catalytic efficacy of the Ni-Pd nanoparticle catalysts, having high Ni to Pd atomic ratios, was also investigated for Heck and Sonogashira reactions. The structural and chemical properties of the synthesised Ni-Pd nanoparticles were investigated by TEM, SEM, EDX, P-XRD, XPS and ICP-AES analyses. ICP-AES and XPS analyses were performed to study the Pd leaching behaviour and to establish the stability of the studied Ni-Pd nanoparticle catalysts. Moreover, first principles calculations were performed using icosahedral Ni_{55-x}Pd_x (x = 0, 1, 3 and 6) clusters to assess the possible Ni to Pd charge transfer by estimating the net negative charge accumulation on Pd atoms.

2. Results and discussion

View Article Online
DOI: 10.1039/C6CY00037A

2.1. Synthesis and Characterization of Ni-Pd nanoparticle catalysts. We first prepared bimetallic $\text{Ni}_{0.99}\text{Pd}_{0.01}$ and $\text{Ni}_{0.95}\text{Pd}_{0.05}$ nanoparticles by following our previously reported aqueous-based reduction procedure, where the aqueous solutions containing an adequate molar ratio of nickel and palladium salts was added an aqueous solution of sodium borohydride in the presence of polyvinylpyrrolidone (PVP) to obtain Ni-Pd nanoparticles as black suspension.¹² Analogously, monometallic Ni and Pd nanoparticle were also prepared from the respective metal salts. The morphological, electronic and compositional information of the synthesised bimetallic Ni-Pd nanoparticles were obtained by using powder XRD, XPS, ICP-AES, electron microscopy (TEM and SEM), energy dispersive X-ray spectroscopy (EDX) and elemental mapping. As inferred from the TEM and high angle annular dark field scanning TEM (HAADF-STEM) images shown in Fig. 1 and 2 (Fig. S1 and S2 of the ESI†), the average particle size of $\text{Ni}_{0.99}\text{Pd}_{0.01}$ and $\text{Ni}_{0.95}\text{Pd}_{0.05}$ nanoparticles is *ca.* 10 nm. The cross sectional composition line scan EDX profile of the Ni-Pd nanoparticles, as shown in Fig. 1 and 2, inferred the presence of both the metals (Ni and Pd) with no sign of segregation, suggesting the alloy composition of the bimetallic Ni-Pd nanoparticles. Further, the TEM-EDX point analysis inferred a uniform composition of the Ni-Pd nanoparticles (Fig. 1 and 2). Moreover, the elemental mapping of Ni-Pd nanoparticles also supports the presence of both the metals (Ni and Pd), further supporting the uniform composition of Ni-Pd nanoparticles (shown in Fig. 1 and 2). Moreover, ICP-AES analysis for Ni to Pd atomic ratio in $\text{Ni}_{0.99}\text{Pd}_{0.01}$ and $\text{Ni}_{0.95}\text{Pd}_{0.05}$ nanoparticles corresponds well with the proposed compositions.

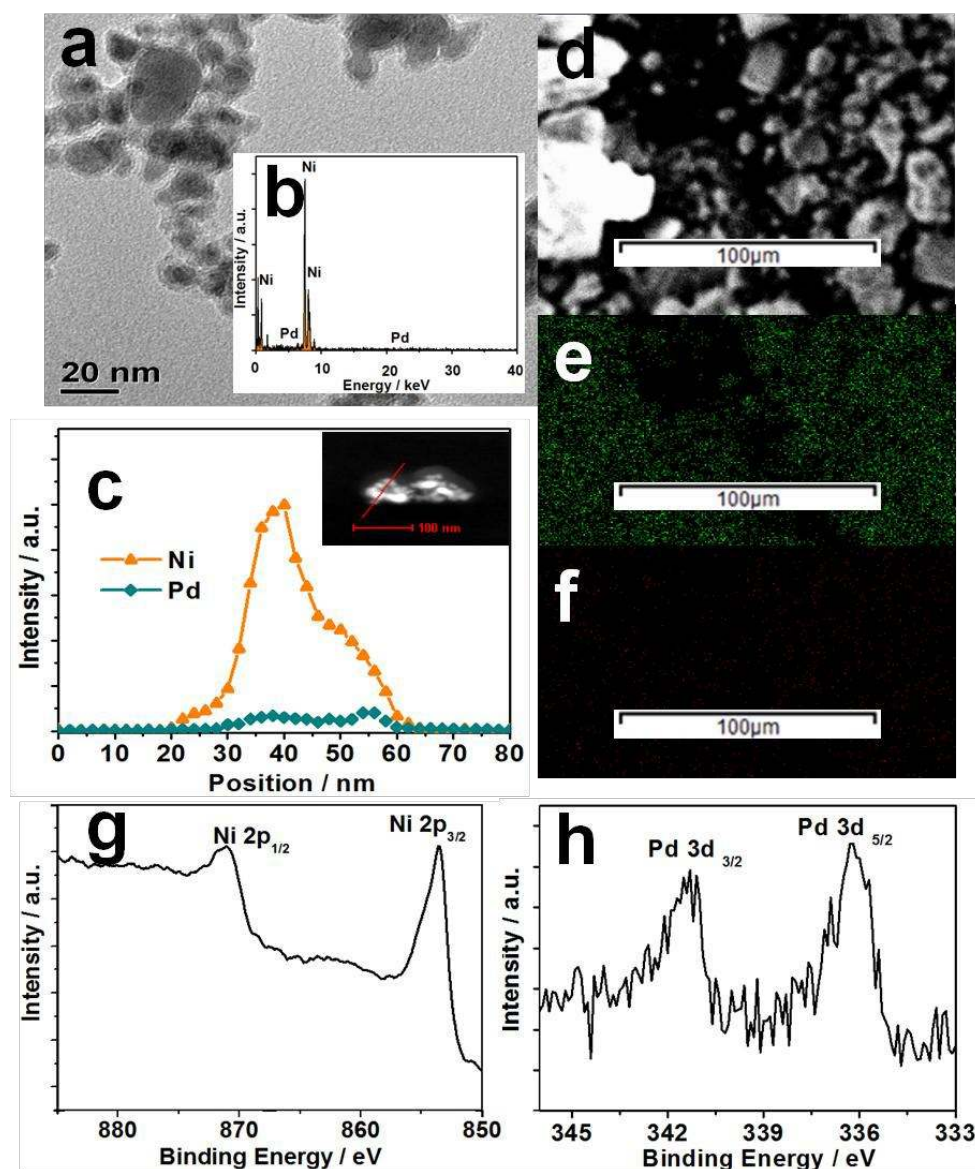


Fig. 1 Characterization of $\text{Ni}_{0.99}\text{Pd}_{0.01}$ nanoparticle catalyst. (a) TEM image. (b) Point scan EDX profile. (c) Line scan compositional profile corresponding to HAADF-STEM image (inset). (d-f) EDX elemental mapping showing (e) Ni (in green) and (f) Pd (in red) elements corresponding to the (d) SEM image. (g-h) XPS profiles of Ni-L and Pd-K edge.

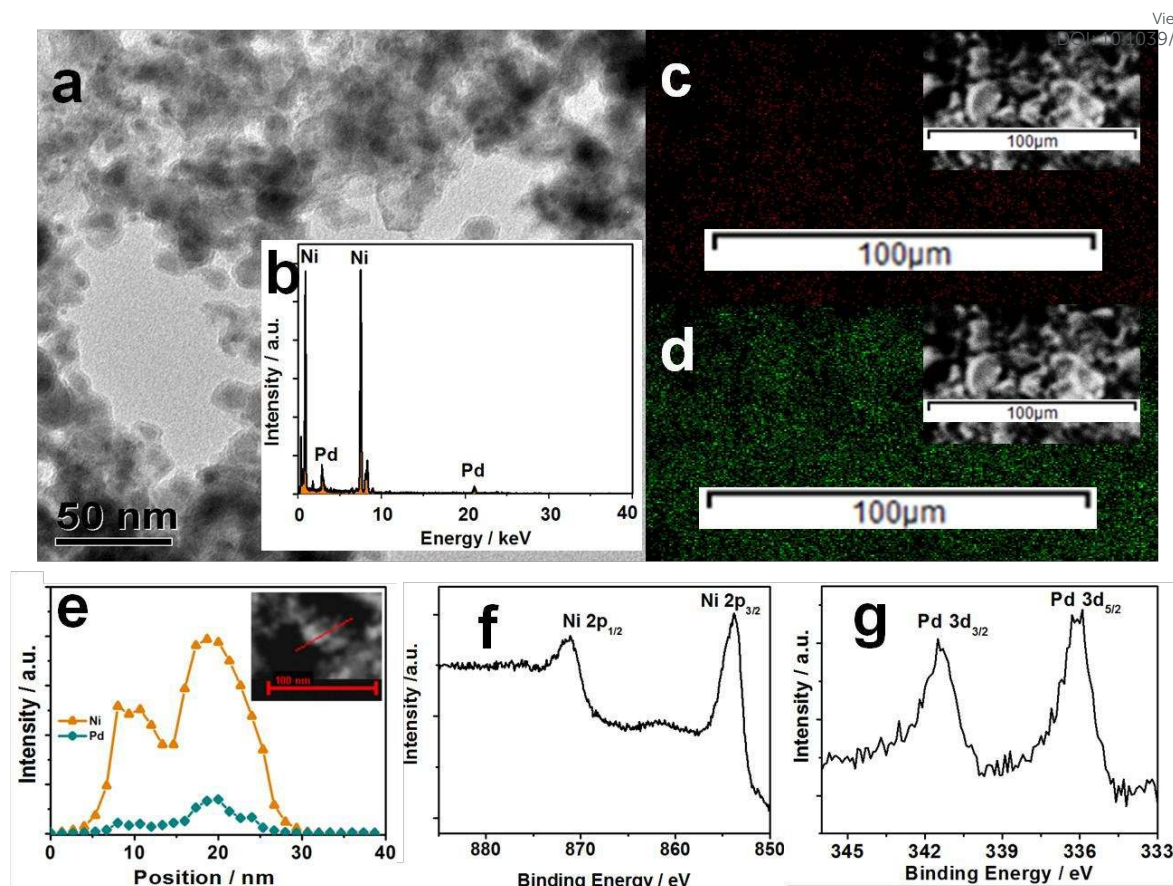


Fig. 2 Characterization of $\text{Ni}_{0.95}\text{Pd}_{0.05}$ nanoparticle catalyst. (a) TEM image. (b) Point scan EDX profile. (c-d) EDX elemental mapping showing (c) Ni (in green) and (d) Pd (in red) elements corresponding to the SEM image (inset). (e) Line scan compositional profile corresponding to HAADF-STEM image (inset). (f-g) XPS profiles of Ni-L and Pd-K edge.

The powder XRD pattern of Ni-Pd nanoparticles displayed a broad prominent peak at 2θ value of 44.44° (for $\text{Ni}_{0.99}\text{Pd}_{0.01}$ nanoparticles) and 43.54° (for $\text{Ni}_{0.95}\text{Pd}_{0.05}$ nanoparticles), corresponding to (111) plane diffraction similar to Ni (JCPDS 04-0850) (Fig. S3 of the ESI†). We performed Le Bail refinement of the powder XRD data of $\text{Ni}_{0.99}\text{Pd}_{0.01}$ and $\text{Ni}_{0.95}\text{Pd}_{0.05}$ nanoparticles to estimate accurate d -spacing values using FullProf program. The d -spacing values calculated from the Le Bail fitting for $\text{Ni}_{0.99}\text{Pd}_{0.01}$ and $\text{Ni}_{0.95}\text{Pd}_{0.05}$ (Fig. S4 of the ESI†) for the (111) planes of the face-centered cubic (*fcc*) are 0.203 nm and 0.207 nm, respectively.

The lattice constant for $\text{Ni}_{0.99}\text{Pd}_{0.01}$ and $\text{Ni}_{0.95}\text{Pd}_{0.05}$ nanoparticles are averaged at 3.5276 \AA and 3.6006 \AA , respectively, compared to pure Ni (3.524 \AA) and Pd (3.873 \AA), ensuring the alloy formation where the lattice expansion occurs due to the substitution of Ni by Pd atoms in the Ni-Pd nanoparticles. In consistence with the TEM and XRD results, the appearance of characteristic signals corresponding to the metallic Ni 2p and Pd 3d in the XPS analysis of Ni-Pd nanoparticles (as shown in Fig. 1g-1h and 2f-2g), indicating the coexistence of both the metals in the bimetallic Ni-Pd nanoparticles. For $\text{Ni}_{0.99}\text{Pd}_{0.01}$ nanoparticles, the XPS signals corresponding to the metallic Ni^0 (Ni 2p_{3/2} core level) and Pd^0 (Pd 3d_{5/2} core level) were observed at 853.54 eV and 336.35 eV, respectively. Analogously, the signals appeared at 853.81 eV and 336.44 eV in the XPS analysis of the $\text{Ni}_{0.95}\text{Pd}_{0.05}$ nanoparticle catalyst, can be assigned to the metallic Ni^0 (Ni 2p_{3/2} core level) and Pd^0 (Pd 3d_{5/2} core level), respectively. Moreover, XPS spectra of the Ni-Pd alloy nanoparticle with Ar sputtering experiment at different time interval (0 ~ 180 min) showed the appearance of representative peaks of Ni and Pd for the spectra (Fig. S5 and S6 of the ESI†).

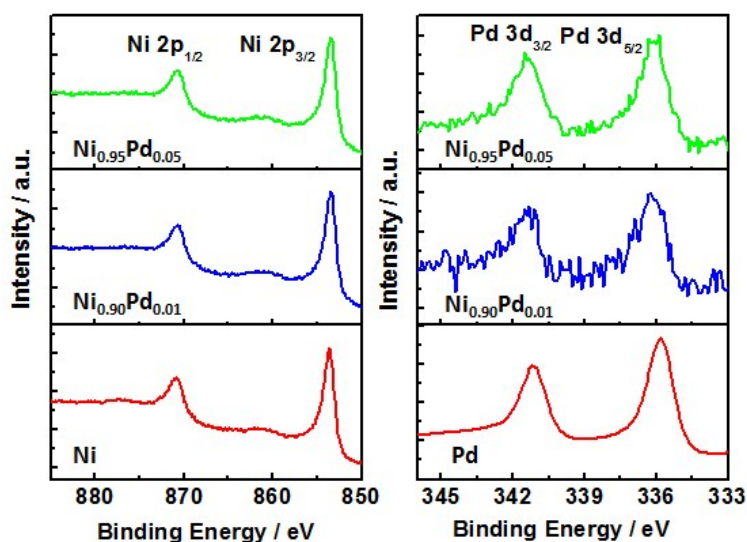


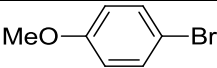
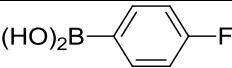
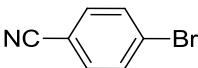
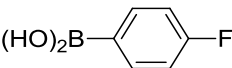
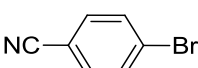
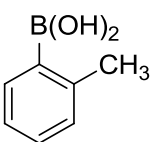
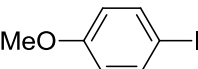
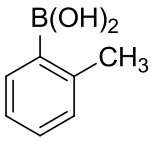
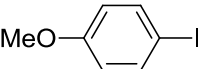
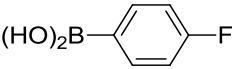
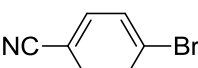
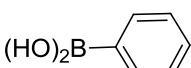
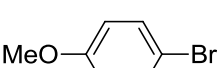
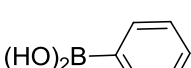
Fig. 3 XPS profiles of Ni-L and Pd-K edges for the fresh Ni, $\text{Ni}_{0.99}\text{Pd}_{0.01}$, $\text{Ni}_{0.95}\text{Pd}_{0.05}$ and Pd nanoparticles.

More significantly, binding energy of the Ni and Pd for Ni-Pd alloy nanoparticle showed shifts compared to those of monometallic Ni and Pd nanoparticles (Fig. 3). Moreover, we also compared the shift in the binding energy of the Pd 3d_{5/2} and Ni 2p_{3/2} core level appeared in the XPS spectra for bimetallic Ni-Pd nanoparticles, ΔE , relative to those for monometallic Pd (335.8 eV) and Ni (853.5 eV). For Ni_{0.99}Pd_{0.01} nanoparticles, ΔE for Ni 2p_{3/2} core level is close to zero, and that for Pd 3d_{5/2} is +0.5 eV. Similarly for Ni_{0.95}Pd_{0.05} nanoparticles, ΔE for Ni 2p_{3/2} is +0.2 eV and for Pd 3d_{5/2} is +0.6 eV. These results inferred that shift in binding energies, ΔE , for Ni 2p_{3/2} core levels are not significant, presumably due to the higher content of Ni in these Ni-Pd alloys the effect of possible charge transfer or lattice strain is dispersed. However, due to the very low content of Pd in the studied Ni-Pd nanoparticles, any electronic or bonding disturbance will be highlighted more prominently, as inferred from the large positive shifts (ΔE) observed for Pd 3d_{5/2} core levels for bimetallic Ni-Pd nanoparticles. Although, binding energy for alloyed Pd shows positive shift than of pure Pd, indicating at first glance that a partial positive charge localized on Pd atom. However, XPS binding energy shifts, particularly in alloys, are caused not only by chemical shifts but also by several other factors including lattice disturbance due to alloying.¹⁵ Therefore, the observed shift in Pd 3d_{5/2} binding energy is ascribed to the lattice contraction of Pd atoms resulted from the inclusion of Ni atoms due Ni-Pd alloy formation. Analogous positive shifts in binding energies of Pd 3d_{5/2} were also reported earlier by Lu *et al.* and Rao *et al.* in the alloy Ni-Pd bimetallic nanoparticles.^{15b,c} It is worthy to mention that appearance of Ni and Pd at the same time of the Ar sputtering and the observed shifts in the XPS spectra strongly support the alloy composition of the Ni-Pd nanoparticles.

2.2. Investigation of Ni-Pd nanoparticle catalyzed Suzuki-Miyaura reaction. The reactivity of the synthesised Ni-Pd nanoparticle catalyst for the Suzuki-Miyaura reaction of arylhalides with arylboronic acid was explored under the optimized

reaction condition,¹² and the results are presented in Table 1. As inferred from the results shown in Table 1, good to excellent yields of the biaryls products (Table 1, entries 1-7) can be achieved with Ni-Pd nanoparticles at room temperature or 50 °C in water-ethanol solution. Notably, our results indicated that the reported Ni-Pd nanoparticle catalysts work significantly well for a wide range of arylbromides/iodides with substituted (Table 1, entries 1-5) and un-substituted (Table 1, entries 6-7) arylboronic acids, to obtain the corresponding biaryl products in excellent yields.

Table 1 Suzuki reaction catalyzed by Ni-Pd alloy nanoparticle catalyst. ^a

Entry	Arylhalide	Arylboronic acid	Yield (%) / Time (h) ^b	Yield (%) / Time (h) ^c
1			73/6	75/7
2			85/2	84/2.5
3			89/9.5	90/10.5
4 ^d			89/8	90/5
5 ^d			90/7	92/3
6			91/2	92/1.5
7			90/2.5	91/2

^a Reaction conditions: arylboronic acid (1.2 mmol), arylbromide (1.0 mmol), K₂CO₃ (2.0 mmol), H₂O-C₂H₅OH (1:1 v/v, 20 mL), catalyst (2 mol %), 50 °C. ^b Isolated yields with

Ni_{0.99}Pd_{0.01} nanoparticle catalysts. ^c Isolated yields with Ni_{0.95}Pd_{0.05} nanoparticle catalysts. View Article Online
DOI: 10.1039/C6CY00037A

^dFor aryl iodide: NaOH (2.0 mmol), room temperature.

To further explore the catalytic performance of Ni-Pd nanoparticles and to compare it with monometallic Ni and Pd nanoparticle catalyst, Suzuki-Miyaura reaction of 4-iodoanisole and 2-methylboronic acid in water-ethanol solution was performed in standardised reaction conditions.¹² Results presented in Fig. 4 inferred the superior catalytic activity of the Ni-Pd nanoparticle catalyst in contrast to the monometallic Ni and Pd nanoparticle catalysts. Moreover, the catalytic reaction performed with 0.1 mol% Pd nanoparticle catalyst (which is equal to the Pd content in 2 mol% of Ni_{0.95}Pd_{0.05} nanoparticle catalyst) or even with 2 mol% Pd revealed a very poor activity towards the coupled product (Fig. 4).¹² Moreover, a strong dependence of catalytic performance of Ni-Pd nanoparticle catalyst on the Ni to Pd atomic ratio was also observed, where with the increase in the Ni content catalytic activity of the resulting Ni-Pd nanoparticle catalyst also increases.

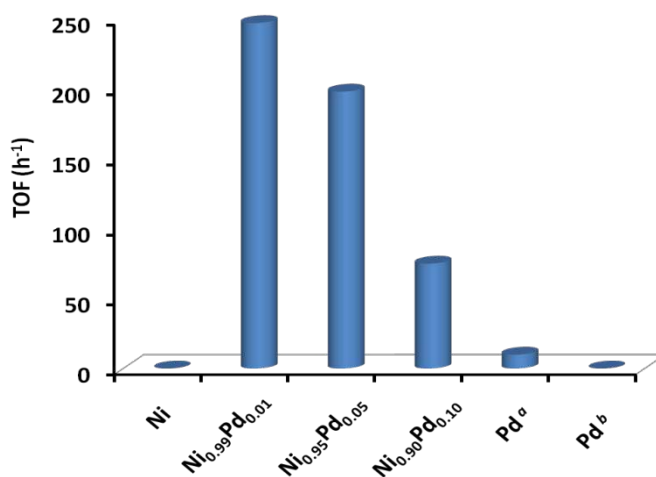


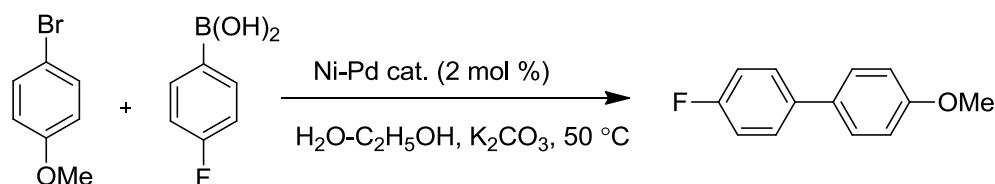
Fig. 4 Comparison of catalytic conversions for cross-coupled product in the Suzuki-Miyaura reaction of 4-iodoanisole and 2-methylphenylboronic acid in presence of 2 mol% of various catalysts, at room temperature in water-ethanol solution (5 h). ^a Reaction with 2 mol% Pd

nanoparticle catalyst (5 h). ^b Reaction with 0.1 mol% Pd, equal to the Pd content present in highly active 2 mol% Ni_{0.95}Pd_{0.05} nanoparticle catalyst (5 h).

View Article Online
DOI: 10.1039/C6CY00037A

The highest catalytic activity was achieved with Ni_{0.99}Pd_{0.01} nanoparticle catalyst and the catalytic efficacy, in terms of TOF (h⁻¹), is in the order of Ni_{0.99}Pd_{0.01} > Ni_{0.95}Pd_{0.05} > Ni_{0.90}Pd_{0.10} (Fig. 4 and Table 2). Notable, Suzuki-Miyaura reaction of 4-bromoanisole with 4-fluoroboronic acid performed at 50 °C showed more prominent effect of varying the Ni to Pd atomic ratios in the Ni-Pd nanoparticles on their catalytic activities (Table 2). TONs reaching 3.6 x 10³ can be achieved with Ni_{0.99}Pd_{0.01} nanoparticle catalysts (Table 2). These results are consistent with our previous findings where an increase in the activity of Ni-Pd nanoparticle catalyst was observed with an enhancement in Ni to Pd molar ratio in the Ni-Pd nanoparticle catalyst.¹²

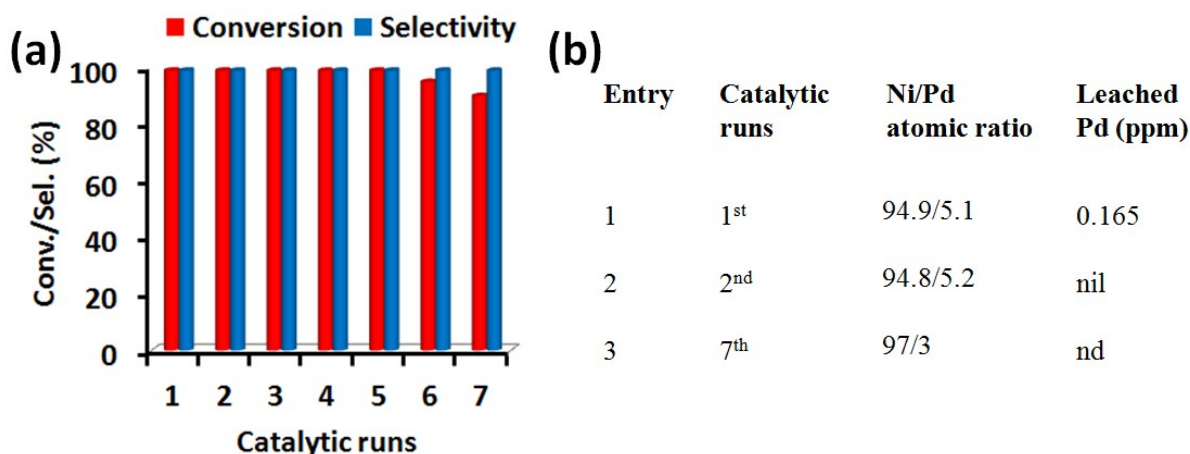
Table 2 Influence of Ni to Pd atomic ratio on the catalytic activity of Ni-Pd nanoparticle catalysts for Suzuki-Miyaura reaction. ^a



Entry	Catalyst	Conv./Sel. (%) ^b	TON/TOF (h ⁻¹)
1	Ni _{0.99} Pd _{0.01}	72/99	3600/3600
2	Ni _{0.95} Pd _{0.05}	54/99	540/540
3	Ni _{0.90} Pd _{0.10}	15/99	75/75

^a Reaction condition: 4-bromoanisole (1.0 mmol), 4-fluoroboronic acid (1.2 mmol), K₂CO₃ (2 mmol), H₂O-C₂H₅OH (1:1 v/v, 20 mL), 50 °C, 1 h. ^b Conversion and selectivity were determined by ¹H NMR.

The observed results clearly inferred the direct involvement of the Ni in the bimetallic nanoparticles which shows the strong synergistic effect in the Ni-Pd nanoparticle catalyst.¹⁶ A possible explanation for the superior catalytic activity of Ni-Pd nanoparticles is that a charge transfer from Ni to Pd making the Pd centre electron rich, a favourable site for oxidative addition of arylhalide. Such kind of charge transfer or redistribution can be expected in Ni-Pd



nanoparticle with even higher Ni to Pd atomic ratio. A consequence of such a large volume of charge transfer from Ni to Pd may result in a highly electron rich Pd and therefore could contribute to the superior catalytic activity of Ni_{0.99}Pd_{0.01} nanoparticle catalyst.

Fig. 5 (a) Recyclability of Ni_{0.95}Pd_{0.05} alloy nanoparticle catalyst with 4-iodoanisole and 2-methylphenylboronic acid at room temperature. (b) ICP-AES data of the Ni_{0.95}Pd_{0.05} nanoparticle catalyst.

To further investigate the nature of the active catalytic species, a series of experiments including recyclability experiments, catalyst poisoning test and leaching experiments were performed for the Ni-Pd nanoparticle catalyzed Suzuki-Miyaura reaction. Stability and robustness of the catalyst was examined by reusing the Ni-Pd nanoparticle catalyst several times for the catalytic Suzuki-Miyaura reaction of 2-methylphenylboronic acid and 4-iodoanisole at room temperature. The catalyst recovered by centrifugation and successively

used for at least seven consecutive catalytic cycles without any significant loss in the catalytic activity (Fig. 5). The reused catalyst does not show any significant change in the Ni to Pd atomic ratio due to no or negligible Pd leaching for the Ni-Pd nanoparticle catalyst, as inferred from the ICP-AES analysis (Fig. 5 and Table S1 of the ESI†). Moreover, the XPS measurements for the Ni-Pd nanoparticle catalysts analysed before and after the catalytic reaction does not show any significant compositional or electronic distortion of either or both the metallic components (Ni or Pd) in the Ni-Pd nanoparticle catalyst (Fig. S7 of the ESI†). These results further inferred the high aqueous-aerobic stability of the studied Ni-Pd nanoparticles catalyst. To investigate further the stability of the Ni_{0.95}Pd_{0.05} nanoparticle catalyst, supernatant and recovered catalyst of the 1st and 2nd cycle was analyzed by ICP-AES (Table S1 of the ESI†). Results were indeed encouraging, as nearly no Pd leaching was observed for the first two consecutive catalytic runs. Moreover, Ni to Pd atomic ratios of the recovered catalyst matched well with those of fresh catalyst, which indicated that the composition of the Ni-Pd nanoparticle catalysts remains intact during the catalytic reaction (Table S1 of the ESI†). Interestingly, ICP-AES analysis of the Ni_{0.95}Pd_{0.05} nanoparticle catalyst recovered after 7th catalytic cycle showed only a minor change in Ni to Pd atomic ratio suggesting that the Ni-Pd nanoparticle catalyst is stable. Furthermore, the Ni_{0.99}Pd_{0.01} and Ni_{0.95}Pd_{0.05} nanoparticle catalysts also remain stable under elevated temperature (50 °C), as the recovered catalysts showed no significant change in Ni to Pd atomic ratio with negligible or absence of Pd leaching (Table S1 of the ESI†). Moreover, catalyst poisoning test performed with an excess amount of Hg, resulted in a significant decrease in the catalytic activity (< 10% conversion) of the Ni-Pd nanoparticle catalyst, which demonstrated the heterogeneous nature of Ni-Pd nanoparticle catalysts.

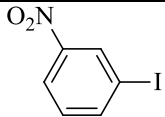
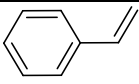
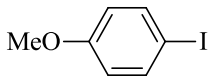
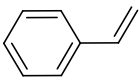
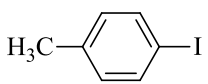
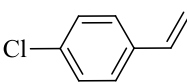
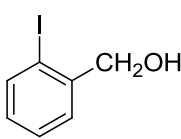
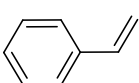
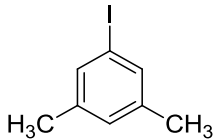
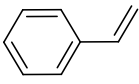
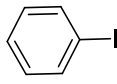
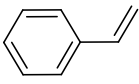
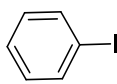
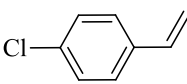
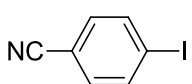
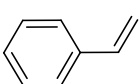
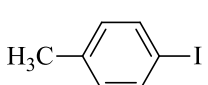
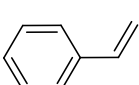
The detailed ICP-AES analyses of the fresh and the spent Ni-Pd nanoparticle catalysts recovered from the Suzuki-Miyaura reaction, clearly inferred the advantageous role of the

high contents of Ni in the Ni-Pd catalyst to suppress the Pd leaching and enhancing the catalyst stability. Presumably, the high contents of Ni in Ni-Pd nanoparticle catalysts stimulate the ligand effect by transferring electron density to Pd atoms, which imparts more negative charge on Pd atoms. The electron rich Pd atoms facilitate faster oxidative addition of arylhalides and therefore enhanced catalytic activity of the Ni-Pd nanoparticle catalysts. Moreover, the negligible leaching of the Pd in the Ni-Pd nanoparticle catalyst can be employed for synthesis of biologically active component through C-C coupling reaction.¹⁷

2.2. Extension to Ni-Pd catalyzed other C-C cross coupling reactions.

Encouraged with the observed superior catalytic activity of Ni-Pd nanoparticle catalyst for Suzuki-Miyaura reaction, the scope and activity of the Ni-Pd nanoparticle catalysts, containing high Ni to Pd atomic ratio, were also investigated for other analogous C-C cross coupling reactions (Heck and Sonogashira reactions). After establishing the most suitable reaction condition for the Ni-Pd nanoparticle catalyzed Heck reaction of 4-iodotoluene with styrene by screening various bases (K_2CO_3 , K_3PO_4 and $(C_2H_5)_3N$) and solvent (H_2O -DMF and H_2O - C_2H_5OH) (Table S2 of the ESI[†]), catalytic Heck reaction using various aryl iodides and arylalkenes was performed in H_2O -DMF at 80 °C in 24 h to obtain moderate to good yields for the coupled products. Results are summarised in Table 3. Notably, aryl iodides containing both electron donating (Table 3, entries 2-5, 9) and electron withdrawing (Table 3, entries 1, 8) substituents can be effectively involved in the coupling reaction with styrene and substituted styrene to yield substituted cross-coupled products. Arylbromides were also employed for Heck reaction, under modified reaction conditions, and high to good conversions with moderate to poor selectivities and yields for the cross-coupled product were observed (Table S3 of the ESI[†]).

Table 3 Substrate scope for Ni_{0.95}Pd_{0.05} catalyzed Heck reaction. ^a

Entry	Arylhalides	Arylalkenes	Time (h)	Yields (%) ^b
1			24	59
2			24	72
3			24	76
4			24	65
5			24	49
6			9	48
7			9	50
8			24	48
9			24	59

^a Reaction condition: arylhalides (1.0 mmol), arylalkenes (1.5 mmol), K₂CO₃ (2.0 mmol), H₂O-DMF (1:1 v/v, 5 mL), catalyst (2 mol%), 80 °C. ^b Isolated yields.

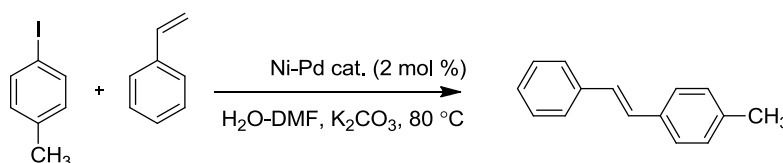
Further to explore the effect of Ni to Pd atomic ratio on the catalytic activity of Ni-Pd nanoparticle catalyst for Heck reactions, catalytic reactions were performed using 4-

iodotoluene with styrene in the presence of various Ni-Pd nanoparticle catalysts (Table 4).

View Article Online
DOI: 10.1039/C6CY00037A

Consistent with the trends obtained with the Suzuki-Miyaura reaction, a significant enhancement in the catalytic activity of the Ni-Pd nanoparticle with the increase in Ni to Pd atomic ratio was also observed for the Heck reaction. The catalytic activities are in the order of Ni_{0.99}Pd_{0.01} (TOF 183 h⁻¹) > Ni_{0.95}Pd_{0.05} (TOF 38 h⁻¹) > Ni_{0.90}Pd_{0.10} (TOF 28 h⁻¹) (Table 4). TONs up to 2.6 × 10³ can be achieved for the Heck reaction of 4-iodotoluene and styrene with Ni_{0.99}Pd_{0.01} nanoparticle catalysts in H₂O-DMF at 80 °C. It is worth mentioning here, that the monometallic Ni nanoparticle catalysts are inactive for the Heck reaction under analogous reaction condition (Fig. S8 of the ESI[†]), further support the synergistic interaction between Ni and Pd has a significant impact on the improved catalytic activity of Ni-Pd nanoparticle catalyst.

Table 4 Influence of Ni to Pd atomic ratio on the catalytic activity of Ni-Pd nanoparticle catalysts Heck reaction. ^a



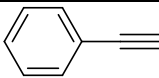
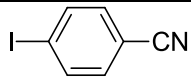
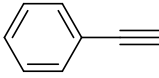
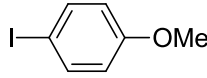
Entry	Catalyst	TON/TOF (h ⁻¹) ^b
1	Ni _{0.99} Pd _{0.01}	2575/183.9
2	Ni _{0.95} Pd _{0.05}	537/38.35
3	Ni _{0.90} Pd _{0.10}	395/28.2

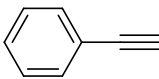
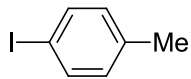
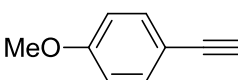
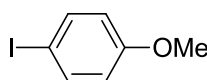
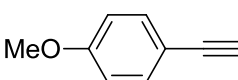
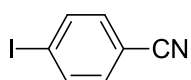
^a Reaction condition: 4-iodotoluene (1.0 mmol), styrene (1.5 mmol), K₂CO₃ (2.0 mmol), H₂O-DMF (1:1 v/v, 5 mL), 80 °C, 14 h. ^b Determined by ¹H NMR.

Catalytic activity of the Ni-Pd nanoparticle catalysts was also explored for the Sonogashira reaction of arylhalide with arylalkyne in H₂O-DMF in the presence of K₂CO₃ at

80 °C, and the results are shown in the Table 5. Results inferred that reaction with electron withdrawing arylhalides (Table 5, entries 1, 5) gave moderately good yields (56-65%), whereas electron donating arylhalides (Table 5, entries 2-4) resulted in only poor yields (26-36%). In contrary to arylhalides, substituents of arylalkyne have less prominent effect on the yields of the coupled products (Table 5, entries 4, 5). Moreover, performing Sonogashira reaction in the presence of Cu(I) as a co-catalyst, resulted in the formation of homocoupled product of arylalkyne and hence decrease the yields of the desired cross coupled products (Table S4 of the ESI†). The influence of Ni-Pd nanoparticle catalyst with various Ni to Pd atomic ratios was also examined for Sonogashira reaction of 4-iodotoluene with phenylacetylene in H₂O-DMF at 80 °C (Table 6 and Fig. S9 of the ESI†). Consistent with the trends of the catalytic activity observed for Suzuki-Miyaura and Heck reactions with Ni-Pd nanoparticle catalyst with the varying Ni to Pd atomic ratio, Ni-Pd nanoparticle catalysts having high Ni to Pd atomic ratio were also found to be more active than those with low Ni to Pd atomic ratio for the Sonogashira reaction. Moreover, reactions with aryl bromide under analogous or modified reaction conditions, resulted in good to moderate conversions with moderate to poor selectivities and yields for the cross-coupled products (Table S5 of the ESI†).

Table 5 Sonogashira reaction with Ni_{0.95}Pd_{0.05} alloy nanoparticle catalyst. ^a

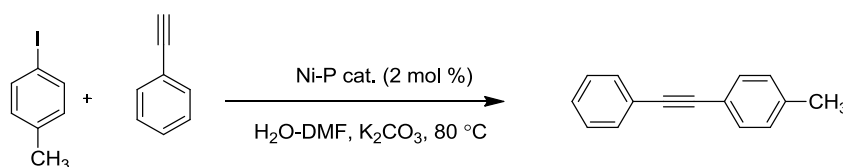
Entry	Arylalkyne	Aryliodides	Time (h)	Yield (%) ^b
1			24	55
2			24	26

3			24	36
4			24	30
5			20	65

View Article Online
DOI: 10.1039/C6CY00037A

^a Reaction conditions: arylalkyne (1.0 mmol), aryl iodide (1.0 mmol), K₂CO₃ (2.0 mmol), catalyst (2 mol %) in H₂O-DMF (1:1 v/v, 5 mL), 80 °C. ^b Isolated yields.

Table 6 Influence of Ni to Pd atomic ratio on the catalytic activity of Ni-Pd nanoparticle catalysts Sonogashira reaction. ^a



Entry	Catalyst	TON/TOF (h ⁻¹) ^b
1	Ni _{0.99} Pd _{0.01}	1575/131
2	Ni _{0.95} Pd _{0.05}	420/35

^a Reaction condition: arylalkyne (1.0 mmol), aryl iodide (1.0 mmol), K₂CO₃ (2.0 mmol), H₂O-DMF (1:1 v/v, 5 mL), catalyst (2 mol %), 80 °C, 12 h. ^b Determined by ¹H NMR.

According to the most acceptable reaction pathway for Pd catalyzed C-C coupling reaction, active Pd species leach out from Pd nanoparticle catalyst, as a result of oxidative addition of arylhalide to generate active soluble Pd²⁺ species (Pd⁰ → Pd²⁺). Later, Pd re-deposited on the catalyst or remains as a ligand-free soluble Pd⁰ species (Pd²⁺ → Pd⁰). We observed that alloying Ni with Pd to form bimetallic Ni-Pd nanoparticle catalysts was found

to be highly beneficial, where the significant Ni to Pd synergic interaction not only significantly contributed to achieve enhanced catalytic activity for C-C coupling reactions, but also enhances the stability of the Ni-Pd nanoparticle catalysts by retarding Pd leaching.

View Article Online
DOI: 10.1039/C6CY00037A

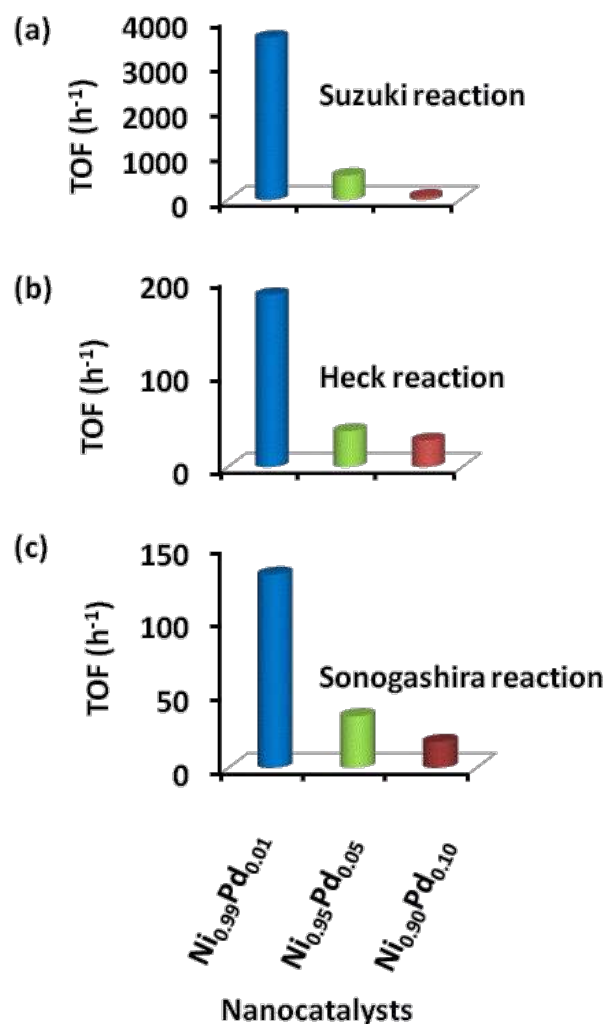


Fig. 6 Comparative TOFs (h^{-1}) of $\text{Ni}_{0.99}\text{Pd}_{0.01}$, $\text{Ni}_{0.95}\text{Pd}_{0.05}$ and $\text{Ni}_{0.90}\text{Pd}_{0.10}$ nanoparticle catalyst for, (a) Suzuki reaction with 4-bromoanisole and 4-fluoroboronic acid at 50 °C in $\text{H}_2\text{O}-\text{C}_2\text{H}_5\text{OH}$ (1:1 v/v, 20 mL) for 1 h. (b) Heck reaction with 4-iodotoluene and styrene at 80 °C in $\text{H}_2\text{O}-\text{DMF}$ (1:1 v/v, 5 mL) for 14 h. (c) Sonogashira reaction with 4-iodotoluene and phenylacetylene at 80 °C in $\text{H}_2\text{O}-\text{DMF}$ (1:1 v/v, 5 mL) for 12 h.

From our study, we reported a remarkable enhancement in the catalytic activity of the Ni-Pd nanoparticle catalysts for C-C coupling reactions achieved by tuning the Ni to Pd

atomic ratio in the bimetallic catalyst (Fig. 6). Ni-Pd nanoparticle catalysts having high Ni to Pd atomic ratio show highest activity, and TOFs up to $3.6 \times 10^3 \text{ h}^{-1}$ were achieved with $\text{Ni}_{0.99}\text{Pd}_{0.01}$ nanoparticle catalyst for Suzuki-Miyaura reactions. Further, to compare the efficiency of our $\text{Ni}_{0.99}\text{Pd}_{0.01}$ catalyst with various other heterogeneous Pd catalysts reported for aqueous based Suzuki reaction, we have tabulated most of these catalysts and compared their TON and TOF (h^{-1}), calculated based on Pd content (Table S6 of the ESI†). Moreover, high catalytic efficacy (TOFs up to $3.6 \times 10^3 \text{ h}^{-1}$) achieved with the studied $\text{Ni}_{0.99}\text{Pd}_{0.01}$ nanoparticle catalyst was also compared with those of the earlier reported bimetallic Ni-Pd heterogeneous catalyst (Fig. S12 of the ESI†). These results inferred that the Ni-Pd nanoparticle catalyst taken into study in the present work, displayed much higher activity than most of the previously reported bimetallic Ni-Pd and monometallic Pd nanoparticle catalytic systems. Analogous enhanced activity was also observed for Heck and Sonogashira coupling reactions with $\text{Ni}_{0.99}\text{Pd}_{0.01}$ nanoparticle catalysts. Considering the position of respective metallic components in the electrochemical series, it can be seen that Ni has lower reduction potential (-0.23 eV) than that of Pd ($+0.83 \text{ eV}$). Therefore, one may expect a natural drift of electronic charge from Ni to Pd, if both the metals are in close proximity. Alloying Ni and Pd provides a favourable environment for the direct interaction between Ni and Pd, and therefore transfer of electron from Ni to Pd. To further determine electronic charge redistribution between Ni and Pd atoms in Ni-Pd alloy nanoparticles, the net charge localization on Ni and Pd atoms was assessed using the icosahedral Ni_{55} , $\text{Ni}_{54}\text{Pd}_1$ (1.8 at% Pd), $\text{Ni}_{52}\text{Pd}_3$ (5.4 at% Pd) and $\text{Ni}_{49}\text{Pd}_6$ (10.9 at% Pd) clusters by first principles calculations.¹⁸⁻²⁰ Bader charge analysis defines atoms in a bimetallic system purely based on electronic charge distribution.²¹ Icosahedral M_{55} cluster was chosen, as this corresponds to a very stable nanocluster with majorly exposed (111) surface,²²⁻²⁶ and is very much in consistent with our experimental findings. Also, due to symmetry constraints, icosahedral Ni_{100} cluster is not possible. Moreover, the next higher analogue of icosahedral cluster will be

View Article Online
DOI: 10.1039/C6CY00037A

of 147 (M_{147}) atoms.²⁷ Therefore we considered icosahedral M_{55} cluster as an ideal model to study the charge distribution in the studied Ni-Pd nanoparticles.

View Article Online
DOI: 10.1039/C6CY00037A

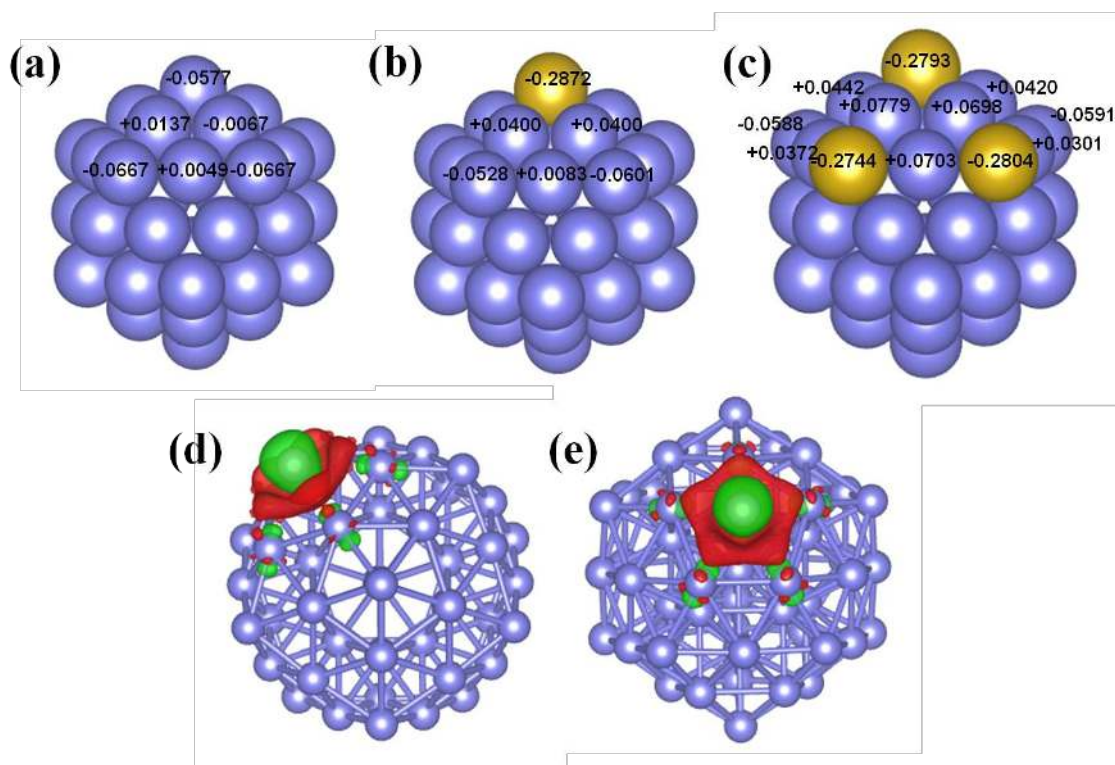
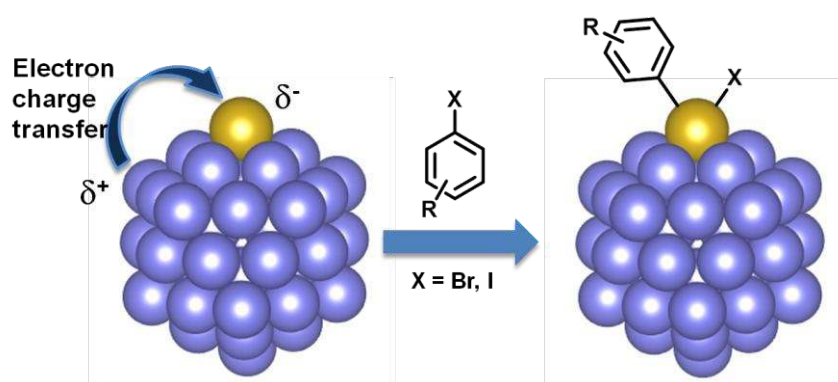


Fig. 7 (a-c) Optimized icosahedral structures of (a) Ni_{55} , (b) $Ni_{54}Pd_1$ and (c) $Ni_{52}Pd_3$ clusters showing the net accumulated charges on Ni (blue) and Pd (golden yellow) atoms. (d-e) The charge density difference (CDD) plots of $Ni_{54}Pd_1$ cluster (Isosurface value = $0.005 e \text{ \AA}^{-3}$), (d) side and (e) top view, showing positive (in red) and negative (in green) charge densities.

The net negative charge accumulation²⁸ occurs predominantly on Pd atoms, whereas Ni atoms were found to be positively charged, suggesting a possible electron charge transfer from Ni to Pd. As two metals with different Fermi levels/electronegativity are brought together, charge will flow from the metal with a lower electronegativity ($Ni = 1.91$) to a higher electronegativity ($Pd = 2.20$), and therefore negative charge densities were observed on Pd atoms. Moreover, having high Ni matrix with very less Pd atoms (as in $Ni_{54}Pd_1$ cluster), such redistribution of charge densities and localization of negative charge densities on Pd atoms are expected to be more prominent. We observed, the negative charge

accumulation is more prominent on Pd atoms for Ni₅₄Pd₁, which is *ca.* 2.94% and *ca.* 3.42% in comparison to Ni₅₂Pd₃ and Ni₄₉Pd₆, respectively. The net average charge on Pd atoms, as depicted in Fig. 7 (Fig. S10 of the ESI†), are in the order of Ni₅₄Pd₁ (-0.2872) > Ni₅₂Pd₃ (-0.2790) > Ni₄₉Pd₆ (-0.2777). The charge density difference (CDD) plot (Fig. 7 and Fig. S11 of the ESI†) also shows that the maximum amount of charge transfer occurs for Ni₅₄Pd₁, whereas decreases with higher Pd concentrations (Ni₅₂Pd₃ and Ni₄₉Pd₆).

Interestingly, the order of negative charge accumulation on Pd in Ni_{55-x}Pd_x clusters corresponds very well with the observed trend in catalytic activity of Ni-Pd nanoparticle catalysts which increases with the increase of Ni to Pd atomic ratio (Fig. 6 and 7). These results provide further evidence for the substantial Ni to Pd electron charge transfer in Ni-Pd nanoparticles, where the highly negatively charged Pd atoms are the most favourable site for facile oxidative addition of arylhalides, and hence the significantly enhanced catalytic activities for C-C coupling reactions (Scheme 2).



Scheme 2 Schematic illustration of Ni (blue) to Pd (golden yellow) electron transfer and the oxidative addition of arylhalides on negatively charged Pd atoms in the Ni-Pd nanoparticle catalyst.

3. Conclusion

View Article Online
DOI: 10.1039/C6CY00037A

In summary, we have successfully explored an easy access to highly active Ni-Pd nanoparticle catalyst for various C-C cross coupling reactions. The catalytic activity of the Ni-Pd nanoparticle catalysts exponentially increased with an increase in the Ni to Pd atomic ratio. The TOF (h^{-1}) of the Ni-Pd nanoparticle catalyst decreases in the order of $\text{Ni}_{0.99}\text{Pd}_{0.01} > \text{Ni}_{0.95}\text{Pd}_{0.05} > \text{Ni}_{0.90}\text{Pd}_{0.10}$ for Suzuki-Miyaura reaction, Heck reaction and Sonogashira reaction. We consider that the enhanced catalytic activity of the Ni-Pd nanoparticle catalyst is presumably due to large electronic charge transfer from Ni to Pd, and therefore resulted in negatively charged Pd atoms which subsequently enhance the oxidative addition of arylhalides, a crucial step of C-C coupling reactions. Our first principles calculations using icosahedral $\text{Ni}_{55-x}\text{Pd}_x$ ($x = 0, 1, 3$ and 6) clusters also displayed a predominantly negative charge accumulation on Pd atoms in Ni-Pd clusters, suggesting a substantial Ni to Pd charge transfer. Moreover, introducing high amount of Ni in the Ni-Pd nanoparticle catalyst not only reduced the cost of the catalyst but also suppresses the leaching of the Pd and made it highly recyclable up to 7 catalytic cycles without any significant loss in the catalytic activity. The high recyclability and negligible leaching of Pd in the Ni-Pd nanoparticle catalyst can be employed for synthesis of several biologically active compounds through C-C bond formation. Our attempt through this work will draw attention of the scientific community for the development a class of highly active bimetallic nanoparticle catalysts, so that use of Pd for coupling reactions can be minimised or vanished by introducing a second inexpensive metal (non-noble metals), at the same time gain stability and retain heterogeneous nature of the catalyst.

4. Experimental section

General. High purity metal salts, chemicals were used for the experiments. NMR spectra were recorded on a Bruker Avance 400 (400 MHz) spectrometer. Chemical shifts are

reported in ppm relative to the centre of the singlet at 7.26 ppm for CDCl_3 and centre of triple
at 77.0 ppm for CDCl_3 in ^{13}C NMR. Electron microscopy (TEM and HAADF-STEM)
experiments and elemental analysis (EDX) were performed with a FEI Tecnai F20 ST TEM
(operating voltage 200 kV) equipped with a field emission gun and EDAX EDS X-ray
spectrometer [Si(Li) detecting unit, super ultra thin window, active area 30 mm^2 , resolution
135 eV (at 5.9 keV)]. SEM images and elemental mapping data were collected on Carl Zeiss
supra 55 (operating voltage 15 kV) equipped with OXFORD Instrument EDS X-ray
spectrometer. For TEM and SEM analysis, a few droplets of the nanoparticle suspension
were deposited onto amorphous carbon-coated 400 mesh copper grids and eventually air
dried. Powder XRD measurements were performed on the dried particles on a Rigaku
SmartLab, Automated Multipurpose x-ray Diffractometer at 40 kV and 30 mA using $\text{Cu K}\alpha$
radiation ($\lambda = 1.5418\text{ \AA}$). Le Bail refinements of powder XRD data were performed
considering profile matching with constant scale using FullProf program. ICP-AES analyses
for Ni and Pd (ppm level) were performed using ARCOS (Spectro, Kleve, Germany). XPS
analyses were carried out on a Shimadzu ESCA-3400 X-ray photoelectron spectrometer
using a $\text{Mg K}\alpha$ source (10 kV, 10 mA). All XPS spectra were calibrated by the C 1s peak
(284.6 eV). The Ar sputtering experiments were carried out under the conditions of
background vacuum 3.2×10^{-6} Pa, sputtering acceleration voltage 1 kV.

Catalytic Suzuki-Miyaura reaction. To the reaction flask containing a suspension of freshly
prepared Ni-Pd nanoparticle catalyst (0.02 mmol based on the metal salt used to prepare the
nanoparticles), in water-ethanol solution (1:1 v/v, 20 mL), was added arylboronic acid (1.2
mmol), aryl iodides (1.0 mmol) and NaOH (2.0 mmol), and the reaction content was
magnetically agitated for desired reaction time at room temperature, and for aryl bromides
 K_2CO_3 was used instead of NaOH at 50 °C. Progress of the reaction was monitored by TLC.
After completion, the reaction mixture was centrifuged at 7000 rpm, to separate out the
catalysts. The reaction mixture was extracted by dichloromethane ($3 \times 10\text{ mL}$) and the

organic layer was dried over anhydrous Na_2SO_4 , which was filtered off, and solvent was evaporated at reduced pressure. All the products were characterised by ^1H and ^{13}C NMR. View Article Online
DOI: 10.1039/C6CY00037A

General procedure for Heck/Sonogashira reaction. To the reaction flask containing a suspension of freshly prepared Ni-Pd nanoparticle catalyst (0.02 mmol based on the metal salt used to prepare the nanoparticles), in H_2O -DMF (1:1 v/v, 5 mL), was added arylalkene (1.5 mmol) or arylacetylene (1.0 mmol) along with arylhalides (1.0 mmol) and K_2CO_3 (2.0 mmol), and the reaction content was magnetically agitated for desired reaction time at 80°C . Progress of the reaction was monitored by TLC. After completion, the reaction mixture was centrifuged at 7000 rpm, to separate out the catalysts. The reaction mixture was extracted by dichloromethane (3×10 mL) and the organic layer was dried over anhydrous Na_2SO_4 , which was filtered off, and solvent was evaporated at reduced pressure. All the products were characterised by ^1H and ^{13}C NMR.

Computational Details. The first-principles calculations are performed using projected augmented wave (PAW) method,¹⁸ as implemented in the Vienna ab initio simulation package (VASP).¹⁹ The exchange-correlation potential is described by using the generalized gradient approximation of Perdew-Burke-Ernzerhof (GGA-PBE).²⁰ Projector augmented wave (PAW) method¹⁸ is employed to treat interactions between ion cores and valence electrons. The structure optimization is done based on the conjugate gradient-minimization scheme under a spin polarization consideration. A $20 \times 20 \times 20 \text{ \AA}^3$ cubic supercell is used to optimize the metal clusters to rule out the possibility of interaction of periodically repeated clusters. The Brillouin zone is sampled using gamma k-point (1×1×1). Plane wave with a kinetic energy cut off of 340 eV is used to expand the electronic wave functions. Bader atomic charges²⁸ are calculated using the Henkelman programme²⁹⁻³¹ to find out the net accumulated charges on the Pd atoms using icosahedral $\text{Ni}_{55-x}\text{Pd}_x$ ($x = 0, 1, 3, 5$) cluster

model with twenty (111) facets. We have used the near-grid algorithm with refine-edge method for the Bader charge analysis.

View Article Online
DOI: 10.1039/C6CY00037A

Acknowledgements

This work is financially supported by IIT Indore, CSIR, New Delhi and SERB (DST), New Delhi. R. K. R. and K. G. thanks CSIR New Delhi, and D. T. thanks UGC New Delhi for their SRF grants. We also thanks SIC, IIT Indore, SAIF, IIT Bombay, IKFT, KIT, Karlsruhe, Germany and AIST, Ikeda, Japan for extended instrumentation facilities.

Keywords: bimetallic; heterogeneous catalysis; nickel-palladium; coupling reactions; electronic charge transfer.

References

- 1 For reviews on synergistic interaction in heterometallic nanoparticles, see: (a) H.-L. Jiang and Q. Xu, *J. Mater. Chem.*, 2011, **21**, 13705-13725; (b) A. K. Singh and Q. Xu, *ChemCatChem*, 2013, **5**, 652-676; (c) D. Wang, Q. Peng and Y. Li, *Nano Res.*, 2010, **3**, 574-580; (d) R. Narayanan, *Molecules*, 2010, **15**, 2124-2138; (e) S. Cai, D. Wang, Z. Niu and Y. Li, *Chin. J. Catal.*, 2013, **34**, 1964-1974; (f) A. Balanta, C. Godard and C. Claver, *Chem. Soc. Rev.*, 2011, **40**, 4973-4985.
- 2 For selected example of synergistic interactions in heterometallic nanoparticles, see: (a) R. Su, R. Tiruvalam, A. J. Logsdail, Q. He, C. A. Downing, M. T. Jensen, N. Dimitratos, L. Kesavan, P. P. Wells, R. Bechstein, H. H. Jensen, S. Wendt, C. R. A. Catlow, C. J. Kiely, G. J. Hutchings and F. Besenbacher, *ACS Nano*, 2014, **8**, 3490-3497; (b) H.-L. Jiang, T. Akita, T. Ishida, M. Haruta, and Q. Xu, *J. Am. Chem. Soc.*, 2011, **133**, 1304-1306; (c) S. K. Singh and Q. Xu, *J. Am. Chem. Soc.*, 2009, **131**, 18032-18033; (d) S. K. Singh and Q. Xu, *Inorg. Chem.*, 2010, **49**, 6148-6152; (e) J. Li, Q.-L. Zhu and Q. Xu, *Catal. Sci. Technol.*, 2015, **5**, 525-530; (f) H. Goksu, S. F.

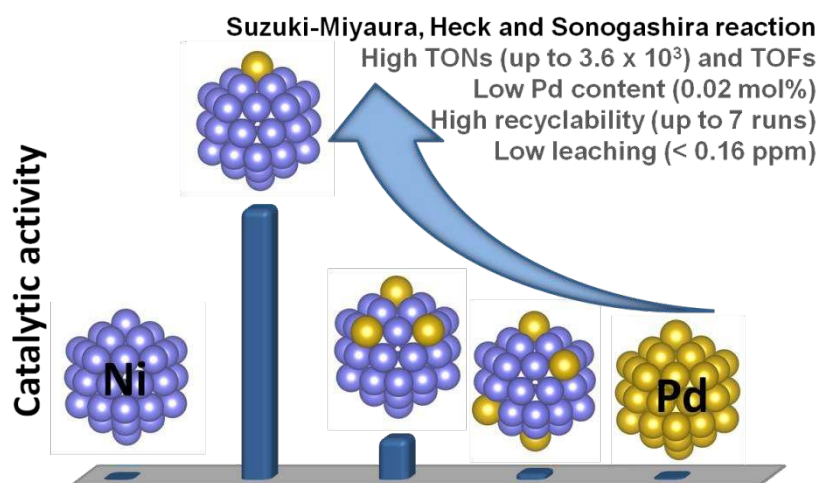
Ho, O. Metin, K. Korkmaz, A. M. Garcia, M. S. Gultekin and S. H. Sun, *ACS Catal.*, 2014, **4**, 1777-1782; (g) M. S. Ahmed and S. Jeon, *ACS Catal.*, 2014, **4**, 1830-1837; (h) Y.-Z. Chen, Y.-X. Zhou, H. Wang, J. Lu, T. Uchida, Q. Xu, S.-H. Yu and H.-L. Jiang, *ACS Catal.*, 2015, **5**, 2062-2069.

- 3 For reviews on Pd catalysed C-C coupling reactions, see: (a) L. X. Yin and J. Liebscher, *Chem. Rev.*, 2007, **107**, 133-173; (b) J. Durand, E. Teuma and M. Gómez, *Eur. J. Inorg. Chem.*, 2008, 3577-3586; (c) R. Ferrando, J. Jellinek and R. L. Johnston, *Chem. Rev.*, 2008, **108**, 846-872; (d) A. Fihri, M. Bouhrara, B. Nekoueishahraki, J.-M. Basseta and V. Polshettiwar, *Chem. Soc. Rev.*, 2011, **40**, 5181-5203; (e) A. Molnar, *Chem. Rev.*, 2011, **111**, 2251-2320; (f) C. Deraedt and D. Astruc, *Acc. Chem. Res.*, 2014, **47**, 494-503.
- 4 For Pd-Au catalysed C-C coupling reactions, see: (a) H. M. Song, B. A. Moosa and N. M. Khashab, *J. Mater. Chem.*, 2012, **22**, 15953-15959; (b) P.-P. Fang, A. Jutand, Z.-Q. Tian and C. Amatore, *Angew. Chem., Int. Ed.*, 2011, **50**, 12184-12188; (c) F. Wang, C. Li, H. Chen, R. Jiang, L.-D. Sun, Q. Li, J. Wang, J. C. Yu and C.-H. Yan, *J. Am. Chem. Soc.*, 2013, **135**, 5588-5601; (d) T. S. A. Heugebaert, S. D. Corte, T. Sabbe, T. Hennebel, W. Verstraete, N. Boon and C. V. Stevens, *Tetrahedron Lett.*, 2012, **53**, 1410-1412; (e) L. Tan, X. Wu, D. Chen, H. Liu, X. Menga and F. Tang, *J. Mater. Chem. A*, 2013, **1**, 10382-10388; (f) M. Nasrollahzadeh, S. M. Sajadi, S. M. Rostami-Vartooni and M. Khalaj, *RSC Adv.*, 2014, **4**, 43477-43484; (g) Q. Xiao, S. Sarina, E. Jaatinen, J. Jia, D. P. Arnold, H. Liuc and H. Zhu, *Green Chem.*, 2014, **16**, 4272-4285; (h) L. Tan, X. Wu, D. Chen, H. Liu, X. Meng and F. Tang, *J. Mater. Chem. A*, 2013, **1**, 10382-10388; (i) M. Nasrollahzadeh, S. M. Sajadi, A. Rostami-Vartoonia and M. Khalaj, *RSC Adv.*, 2014, **4**, 43477-43484.

- 5 For Pd-Ag, Pd-Rh, and Pd-Ru catalysed C-C coupling reactions, see: (a) M. Chen, Z. Zhang, L. Li, Y. Liu, W. Wang and J. Gao, *RSC Adv.*, 2014, **4**, 30914-30922; (b) V. K. Rao and T. P. Radhakrishnan, *J. Mater. Chem. A*, 2013, **1**, 13612-13618; (c) S.-B. Wang, W. Zhu, J. Ke, M. Lin and Y.-W. Zhang, *ACS Catal.*, 2014, **4**, 2298-2306; (d) Md. S. Kutubi, K. Sato, K. Wada, T. Yamamoto, S. Matsumura, K. Kusada, H. Kobayashi, H. Kitagawa and K. Nagaoka, *ChemCatChem*, 2015, **7**, 3887-3894. view Article Online
DOI: 10.1039/C6CY00037A
- 6 For Pd-Co catalysed C-C coupling reactions, see: (a) Y.-S. Feng, X.-Y. Lin, J. Hao and H.-J. Xu, *Tetrahedron*, 2014, **70**, 5249-5253; (b) A. Shaabani and M. Mahyari, *J. Mater. Chem. A*, 2013, **1**, 9303-9311; (c) Y. Li, P. Zhou, Z. Dai, Z. Hu, P. Sun and J. Bao, *New J. Chem.*, 2006, **30**, 832-837; (d) M. B. Thathagar, J. Beckers, G. Rothenberg, *J. Am. Chem. Soc.*, 2002, **124**, 11858-11859; (e) J. A. Coggan, N.-X. Hu, H. B. Goodbrand and T. P. Bender, US Patent, 2006/0025303A1.
- 7 For Pd-Cu catalysed C-C coupling reactions, see: (a) D. Sengupta, J. Saha, G. De and B. Basu, *J. Mater. Chem. A*, 2014, **2**, 3986-3992; (b) M. Korzec, P. Bartczak, A. Niemczyk, J. Szade, M. Kapkowski, P. Zenderowska, K. Balin, J. Lelątko and J. Polanski, *J. Catal.*, 2014, **313**, 1-8; (c) W. Xu, H. Sun, B. Yu, G. Zhang, W. Zhang and G. Gao, *ACS Appl. Mater. Interfaces*, 2014, **6**, 20261-20268; (d) Y.-S. Feng, X.-Y. Lin, J. Hao and H.-J. Xu, *Tetrahedron*, 2014, **70**, 5249-5253; (e) M. Nasrollahzadeh, B. Jalehb and A. Ehsani, *New J. Chem.*, 2015, **39**, 1148-1153; (f) S. Diyarbakir, H. Can and O. Metin, *ACS Appl. Mater. Interfaces*, 2015, **7**, 3199-3206; (g) F. Heshmatpour, R. Abazari and S. Balalaie, *Tetrahedron*, 2012, **68**, 3001-3011.
- 8 For Pd-Ni catalysed C-C coupling reactions, see: (a) Y. Wu, D. Wang, P. Zhao, Z. Niu, Q. Peng and Y. Li, *Inorg. Chem.*, 2011, **50**, 2046-2048; (b) S. U. Son, Y. J. Jang, J. Park, H. B. Na, H. M. Park H. J. Yun, J. Lee and T. Hyeon, *J. Am. Chem. Soc.*, 2004, **126**, 5026-5027; (c) J. Xiang, P. Li, H. Chang, L. Feng, F. Fu, Z. Wang, S.

- Zhang and M. Zhu, *Nano Res.*, 2014, **7**, 1337-1343; (d) M. T. Reetz, R. Breinbauer and K. Wanninger, *Tetrahedron Lett.*, 1996, **37**, 4499-4502; (e) K. Seth, P. Purohit and A. K. Chakraborti, *Org. Lett.*, 2014, **16**, 2334-2337.
- 9 J. Saha, K. Bhowmik, I. Das and G. De, *Dalton Trans.*, 2014, **43**, 13325-13332.
- 10 (a) A. Ohtaka, J. M. Sansano, C. Najera, I. Miguel-Garcia, A. Berenguer-Murcia and D. Cazorla-Amoros, *ChemCatChem*, 2015, **7**, 1841-1847; (b) Ö. Metin, S. F. Ho, C. Alp, H. Can, M. N. Mankin, M. S. Gultekin M. Chi and S. Sun, *Nano Res.*, 2013, **6**, 10-18.
- 11 L. Feng, H. Chong, P. Li, J. Xiang, F. Fu, S. Yang, H. Yu, H. Sheng and M. Zhu, *J. Phys. Chem. C*, 2015, **119**, 11511-11515.
- 12 R. K. Rai, K. Gupta, S. Behrens, J. Li, Q. Xu and S. K. Singh, *ChemCatChem*, 2015, **7**, 1806-1812.
- 13 F. Liao, W. B. T. Lo, D. Sexton, J. Qu, C.-T. Wu and S. C. E. Tsang, *Catal. Sci. Technol.*, 2015, **5**, 887-896.
- 14 Z.-F. Zhao, Z.-J. Wu, L.-X. Zhoy, M.-H. Zhang, W. Li and K.-Y. Tao, *Catal. Commun.*, 2008, **9**, 2191-2196.
- 15 (a) K.S. Kim and N. Winograd, *Chem. Phys. Lett.*, 1975, **30**, 91-95; (b) Q. Zhang, X.-P. Wu, G. Zhao, Y. Li, C. Wang, Y. Liu, X.-Q. Gong and Y. Lu, *Chem. Commun.*, 2015, **51**, 12613-12616; (c) K. R. Harikumar, S. Ghosh and C. N. R. Rao, *J. Phys. Chem. A*, **1997**, 101, 536-540.
- 16 J.-C. Galland, M. Savignac and J.-P. Genet, *Tetrahedron Lett.*, 1999, **40**, 2323-2326.
- 17 C. E. Garrett and K. Prasad, *Adv. Synth. Catal.*, 2004, **346**, 889-900.
- 18 P. E. Blochl, *Phy. Rev. B*, 1994, **50**, 17953-17979.

- 19 (a) G. Kresse and J. Hafner, *Phy. Rev. B*, 1993, **47**, 558-561; (b) G. Kresse and J. Hafner, *Phy. Rev. B*, 1994, **49**, 14251-14269; (c) G. Kresse and D. Joubert, *Phy. Rev. B*, 1999, **59**, 1758-1775. View Article Online
DOI: 10.1039/C6CY00037A
- 20 J. P. Perdew, J. A. Chevary, S. H. Vosko, K. A. Jackson, M. R. Pederson, D. J. Singh and C. Fiolhais, *Phy. Rev. B*, 1992, **46**, 6671-6687.
- 21 W.-X. Ji, C.-W. Zhang, F. Li, P. Li, P.-J. Wang, M.-J. Ren and M. Yuan, *RSC Adv.*, 2014, **4**, 55781-55789.
- 22 J. M. Montejano-Carrizales, M. P. Inñiguez and J. A. Alonso, *J. Cluster Sci.*, 1994, **5**, 287-302.
- 23 Q. Wang, K. H. Lim, S. W. Yang, Y. Yang and Y. Chen, *Theor. Chem. Acc.*, 2011, **128**, 17-24.
- 24 C. Model. Luo, *Simul. Mater. Sci.*, 2002, **10**, 13-20.
- 25 U. Sarkar and S. A. Blundell, *Phy. Rev. B*, 2009, **79**, 125441.
- 26 T. L. Wetzel and A. E. DePristo, *J. Chem. Phys.*, 1996, **105**, 572-580.
- 27 H. Zhang, T. Watanabe, M. Okumura, M. Haruta and N. Toshima, *Nat. Mater.*, 2012, **11**, 49-52
- 28 R. F. W. Bader, *Atoms in Molecules: A Quantum Theory*, Oxford University Press, USA, 1994.
- 29 G. Henkelman, A. Arnaldsson and H. Jonsson, *Comput. Mater. Sci.*, 2006, **36**, 354-360.
- 30 E. Sanville, S. D. Kenny, R. Smith and G. Henkelman, *J. Comput. Chem.*, 2007, **28**, 899-908.
- 31 T. Wang, E. Sanville and G. Henkelman, *J. Phys.: Condens. Matter*, 2009, **21**, 084204.

Table of ContentView Article Online
DOI: 10.1039/C6CY00037A

A facile access to highly active and durable bimetallic Ni-Pd nanoparticle catalysts for Suzuki-Miyaura, Heck and Sonogashira C-C coupling reactions was achieved under moderate reaction condition, wherein an exponential enhancement in TONs/TOFs of the nanoparticle catalysts was observed with an increase in Ni to Pd atomic ratio in the Ni-Pd nanoparticle catalyst owing to a substantial electronic charge transfer from Ni to Pd.